

PHYSICS IN COLLISION - Stanford, California, June 20-22, 2002

## TEST OF GENERAL RELATIVITY: 1995-2002 MEASUREMENT OF FRAME-DRAGGING

Ignazio Ciufolini

*Dip. Ingegneria dell'Innovazione, Università di Lecce, Via Monteroni, 73100 Lecce, Italy*

### ABSTRACT

After an introduction on phenomena due to spin and mass-energy currents on clocks and photons, we review the 1995-2001 measurements of gravitomagnetic field of Earth and Lense-Thirring effect obtained by analyzing the orbits of the two laser-ranged satellites LAGEOS and LAGEOS II; this method has provided a direct measurement of Earth's gravitomagnetism with accuracy of the order of 20 %. A future accurate measurement of the Lense-Thirring effect, at the level of 1% accuracy, may include the LARES experiment that will also provide other basic tests of general relativity and gravitation. Finally, we report the latest measurement of the Lense-Thirring effect, obtained in 2002 with the LAGEOS satellites over nearly 8 years of data. This 2002 result fully confirms and improves our previous measurements of the Earth frame-dragging: the Lense-Thirring effect exists and its experimental value is within  $\sim 20\%$  of what is predicted by Einstein's theory of general relativity.

# 1 Gravitomagnetic phenomena on test gyroscopes, test particles, clocks and photons

In this paper we review some phenomena arising in the vicinities of a rotating body and some proposals and recent measurements of frame-dragging and Lense-Thirring effect obtained by laser-ranged satellites. For a general review of tests and measurements of general relativistic and gravitational effects we refer to [1, 2].

Einstein's general theory of relativity [1] predicts the occurrence of peculiar phenomena on test gyroscopes, test particles, clocks and photons in the vicinity of a mass-energy current and thus in the vicinity of a spinning body due to its rotation.

In section (2) we describe how the orbit of a test-particle is influenced by the spin of a central body and the direct measurement of the orbital perturbations of laser ranged satellites due to the Earth spin, i.e. the Lense-Thirring effect [3]. In 1995-2002 the Lense-Thirring effect was measured with about 20% accuracy using the LAGEOS and LAGEOS II satellites [4, 5, 6, 7], see section (2).

Small test-gyroscopes, that determine the axes of a local, freely falling, inertial frame, where “locally” the gravitational field is “unobservable”, rotate with respect to “distant stars” due to the spin of a body. This effect is described in [1] and should be measured with about 1% accuracy by the Gravity Probe-B experiment [8].

However, not only test particles and gyroscopes are affected by the spin of the central object but also photons and clocks. In this section we review some gravitomagnetic phenomena on clocks and photons. A photon co-rotating around a spinning body takes less time to return to a “fixed point” (with respect to distant stars) than a photon rotating in the opposite direction [1, 9]. Since light rays are used to synchronize clocks, the different travel-time of co-rotating and counter-rotating photons implies the impossibility of synchronization of clocks all around a closed path around a spinning body; the behavior of light rays and the behavior of clocks around a spinning body are intimately connected. In several papers the “frame-dragging clock effect” around a spinning body has been estimated and some space experiments have been proposed to test it [10, 11, 9]. Thus, when a clock, co-rotating very slowly (using rockets) around a spinning body and at a constant distance from it, returns to its starting point, it finds itself advanced relative to a clock kept there at “rest” (with respect to “distant stars”, see above). Similarly a clock, counter-rotating arbitrarily slowly and at a constant distance around the spinning body, finds itself retarded relative to the clock at rest at its starting point [1, 9]. For example, when a clock that co-rotates very slowly around the spinning Earth, at  $r \sim 6000$

km altitude, returns to its starting point, it finds itself advanced relative to a clock kept there at “rest” (with respect to “distant stars”) by  $\Delta\tau \sim \frac{4\pi J_{\oplus}}{r} \sim 5 \times 10^{-17}$  sec, where  $J_{\oplus} \cong 145 \text{ cm}^2$  is the Earth angular momentum. Similarly, a clock, that counter-rotates very slowly around the spinning Earth, finds itself retarded relative to a clock kept there at “rest” by the same amount. Then, the difference between the time read by the two clocks when they meet again after a whole revolution is about  $\sim 10^{-16}$  [9, 11].

However, Einstein’s gravitational theory predicts peculiar phenomena also inside a rotating shell [1]. In reference [9] we derive the time-delay in travel-time of photons due to the spin of a body both outside a rotating body and inside a rotating shell. We then show that this time-delay by the spin of an astrophysical object might be detected in different images of the same source by gravitational lensing.

Since here we are only interested to analyze the time delay due to spin, we chose a simple configuration where source, lens and observer are aligned and we use quasi-Cartesian coordinates [9]. We then get, for a photon with impact parameter  $b$  traveling on the equatorial plane of the source:  $\Delta T = 4 M \ln \left( 2 \frac{\bar{z}}{b} \right) + \frac{4J}{b}$ . In this expression  $\bar{z} \gg b$  is the distance of source and observer from the lens, the first term is the standard Shapiro time delay and the second term is the gravitomagnetic time-delay due to the spin of the deflecting body.

Let us now give the order of magnitude of the time delay due to the spin of some astrophysical sources. For the sun, by considering two light rays on the equatorial plane of the Sun, grazing the Sun on opposite sides, the relative gravitomagnetic time delay is  $\Delta T_{rel}^J = 3.35 \cdot 10^{-12}$  sec. For the lensing galaxy of the Einstein cross, by assuming a simple model for rotation and shape of the central object (see [9] and references therein), we then get:  $\Delta T_{12}^J \simeq 8 \text{ hr}$ . As a third example we consider the relative time delay of photons due to the spin of a typical cluster of galaxies. Depending on the geometry of the system and on the path followed by the photons, we then find relative time delays ranging from a few minutes to several days. Then, at least in principle, one could detect the time delay due to the spin of a lensing galaxy by removing the larger quadrupole-moment time delay by a method described in [9]; of course, as in the case of the Sun, one should be able to accurately enough model and remove all the other delays, due to other physical effects, from the observed time delays between the images.

Let us now analyze the time delay in the travel time of photons propagating inside a shell of mass  $M$  rotating with angular velocity  $\omega$ . Inside a spinning shell it is in general not possible to synchronize clocks all around a closed path. Indeed, if

we consider a clock co-rotating very slowly on the equatorial plane along a circular path with radius  $r$ , when back to its starting point it is advanced with respect to a clock kept there at rest (in respect to distant stars). The difference between the time read by the co-rotating clock and the clock at rest is equal to:  $\delta T = \frac{8M}{3R}\pi\omega r^2$ . For a shell with finite thickness we just integrate this expression from the smaller radius to the larger one.

If we now consider a photon traveling with an impact parameter  $r$  on the equatorial plane of a galaxy; the time delay due to the rotation of the external mass for every infinitesimal shell with mass  $dm = 4\pi\rho R'^2 dR'$  and radius  $R' \geq |r|$ , is [9]:  $\Delta t_{dm} = \frac{8dm}{3}\omega r \frac{\sqrt{R'^2 - r^2}}{R'}$ . This is the time delay due to the spin of the external thin shell. By integrating this expression from  $|r|$  to the external shell radius  $R$ , we have:

$$\Delta T = \frac{32\pi}{3}\omega r \int_{|r|}^R \rho R' \sqrt{R'^2 - r^2} dR' \quad (1)$$

This is the time delay due to the spin of the whole rotating mass of the external shell. From this formula we can easily calculate the relative time delay between two photons traveling on the equatorial plane of a rotating shell, with impact parameters  $r_1$  and  $r_2$ .

Let us give the time delay corresponding to some astrophysical configurations. In the case of the "Einstein cross", after some calculations, based on a standard model for the lensing galaxy (see ref. [9] and references therein), the order of magnitude of the relative time delay of two photons traveling at a distance of  $r_1 \simeq 650 pc$  and  $r_2 \simeq -650 pc$  from the center, using (1) in the case  $r_1 \simeq -r_2$ , is:  $\Delta T \simeq 20$  min. If the lensing galaxy is inside a rotating cluster, or super-cluster, to get an order of magnitude of the time delay due to the spin of the mass rotating around the deflecting galaxy, we use typical super-cluster parameters (see [9] and references therein). If the galaxy is in the center of the cluster and light rays have impact parameters  $r_1 \simeq 15 kpc$  and  $r_2 \simeq -15 kpc$  (of the order of the Milky Way radius), the time delay, applying formula (1) in the case  $r_1 \simeq -r_2$  and  $\rho = constant$ , is:  $\Delta t \simeq 1 day$ .

Finally, if the lensing galaxy is not in the center of the cluster but at a distance  $r = aR$  from the center, with  $0 \leq a \leq 1$  and  $R$  radius of the cluster, by integrating (1) between  $r = aR$  and  $R$ , when  $r_1 \simeq r_2$  we have:

$$\Delta T = \frac{32\pi}{9}\omega(r_1 - r_2)\rho(1 - a^2)^{1/2}(1 - 4a^2)R^3 \quad (2)$$

Thus, if the lensing galaxy is at a distance of 10 Mpc from the center of the cluster, the relative time delay due to the spin of the external rotating mass

between two photons with  $(r_1 - r_2) \simeq 30 \text{ kpc}$ , is:  $\Delta T \simeq 0.9 \text{ day}$ . Since the present measurement uncertainty in the lensing time delay is of the order of 0.5 day [12], the spin time delay might already be observable.

In conclusion, in ref. [9] we have derived and studied the "*spin-time-delay*" in the travel time of photons propagating near a rotating body, or inside a rotating shell due to the angular momentum. We found that there may be an appreciable time delay due to the spin of the body, or shell, thus *spin-time-delay* must be taken into account in the modeling of relative time delays of the images of a source observed at a far point by gravitational lensing. This effect is due to the propagation of the photons in opposite directions with respect to the direction of the spin of the body, or shell. If other time-delays can be accurately enough modeled and removed from the observations [9], one could directly measure the spin-time-delay due to the gravitomagnetic field of the lensing body. We have analyzed the relative time-delay in the gravitational lensing images caused by a typical rotating galaxy, or cluster of galaxies. We have then analyzed the relative spin-time-delay when the path of photons is inside a galaxy, a cluster, or super-cluster of galaxies rotating around the deflecting body; this effect should be large enough to be detected at Earth. The measurement of the spin-time-delay, due to the angular momentum of the external massive rotating shell, might be a further observable for the determination of the total mass-energy of the external body, i.e. of the dark matter of galaxies, clusters and super-clusters of galaxies. Indeed, by measuring the spin-time-delay one can determine the total angular momentum of the rotating body and thus, by estimating the contribution of the visible part, one can determine its dark-matter contribution. The estimates presented in this paper are preliminary because we need to apply the spin-time-delay to some particular, known, gravitational-lensing images. Furthermore, we need to estimate the size and the possibility of modeling other sources of time-delay. Nevertheless, we conclude that, depending on the geometry of the astrophysical system considered, the relative spin-time-delay can be a quite large effect.

## 2 Measurement of gravitomagnetism with laser ranged satellites

In ref. [13] (see also ref. [14]) we describe the LARES experiment to measure the Lense-Thirring effect with relative accuracy of about 1%. This laser ranged satellite, by detecting its perigee rate, would also test the foundations and other basic phenomena of general relativity and gravitational interaction. Indeed, LARES would improve the bounds on hypothetical long-range gravitational forces and the bounds

on deviations from the inverse square law for very weak-field gravity; LARES would improve, by about two orders of magnitude, the accuracy in testing the equivalence principle and would provide an improved measurement in the field of Earth of the PPN (Parametrized-Post-Newtonian) parameters  $\alpha_1$ ,  $\beta$  and  $\gamma$  [13].

In this section we describe the 1995-2002 measurements of the Lense-Thirring effect obtained using LAGEOS and LAGEOS II.

The measurement of distances has always been a fundamental issue in astronomy, engineering, and science in general. So far, laser ranging has been the most accurate technique for measuring the distances to the moon and artificial satellites. Short-duration laser pulses are emitted from lasers on Earth, aimed at the target through a telescope, and then reflected back by optical cube-corner retroreflectors on the moon or an artificial satellite [15], such as LAGEOS. By measuring the total round-trip travel time, one can determine the distance to a retroreflector on the moon with an accuracy of about 2 cm and to the LAGEOS satellites with a few millimeters accuracy.

Our detection and measurement of the Lense-Thirring effect was obtained by using the satellite laser ranging data of the satellites LAGEOS (LAsER GEO-dynamics Satellite, NASA) and LAGEOS II (NASA and ASI, the Italian Space Agency) and the Earth gravitational field models, JGM-3 and EGM-96. The LAGEOS satellites are heavy brass and aluminum satellites, of about 406 kg weight, completely passive and covered with retroreflectors, orbiting at an altitude of about 6,000 km above the surface of Earth. LAGEOS, launched in 1976 by NASA, and LAGEOS II, launched by NASA and ASI in 1992, have an essentially identical structure but they have different orbits. The semimajor axis of LAGEOS is  $a \cong 12,270$  km, the period  $P \cong 3.758$  hr, the eccentricity  $e \cong 0.004$ , and the inclination  $I \cong 109.9^\circ$ . The semimajor axis of LAGEOS II is  $a_{II} \cong 12,163$  km, the eccentricity  $e_{II} \cong 0.014$ , and the inclination  $I_{II} \cong 52.65^\circ$ .

We analyzed the laser-ranging data adopting the IERS (International Earth Rotation Service) conventions [16] in our modeling, however, in the 1998 analysis, we used the static and tidal EGM-96 model [17]. Error analysis of the LAGEOS orbits indicated that the EGM-96 errors can only contribute periodic root-sum-square errors of 2 to 4 mm radially, and in all three directions they do not exceed 10 to 17 mm. The initial positions and velocities of the LAGEOS satellites were adjusted for each 15-day batch of data, along with variations in their reflectivities. Solar radiation pressure, Earth albedo, and anisotropic thermal effects were also modeled [18]. In modeling the thermal effects, the orientation of the satellite spin axis was obtained from ref. [19]. Lunar, solar, and planetary perturbations were also included in the

equations of motion, formulated according to Einstein's general theory of relativity with the exception of the Lense-Thirring effect, which was purposely set to zero. All of the tracking station coordinates were adjusted (accounting for tectonic motions) except for those defining the TRF terrestrial reference frame. Polar motion was also adjusted, and Earth's rotation was modeled from the very long baseline interferometry-based series SPACE96 [20]. We analyzed the orbits of the LAGEOS satellites using the orbital analysis and data reduction software GEODYN II [21].

The node and perigee of LAGEOS and LAGEOS II are dragged by the Earth's angular momentum. From the Lense-Thirring formula [4, 5, 6], we get  $\dot{\Omega}_I^{Lense-Thirring} \cong 31$  mas/yr and  $\dot{\Omega}_{II}^{Lense-Thirring} \cong 31.5$ , where mas is a millisecond of arc. The argument of pericenter (perigee in our analysis),  $\omega$ , also has a Lense-Thirring drag [1], thus, we get for LAGEOS:  $\dot{\omega}_I^{Lense-Thirring} \cong 32$  mas/yr, and for LAGEOS II:  $\dot{\omega}_{II}^{Lense-Thirring} \cong -57$  mas/yr [4, 5, 6]. The nodal precessions of LAGEOS and LAGEOS II can be determined with an accuracy of the order of 1 mas/year. Over our total observational period of about 4 years, we obtained a root mean square (RMS) of the node residuals of about 4 mas for LAGEOS and about 7 mas for LAGEOS II [6]. For the perigee, the observable quantity is the product  $e \cdot a \cdot \dot{\omega}$ , where  $e$  is the orbital eccentricity of the satellite. Thus, the perigee precession  $\dot{\omega}$  for LAGEOS is difficult to measure because its orbital eccentricity  $e$  is  $\sim 4 \times 10^{-3}$ . The orbit of LAGEOS II is more eccentric, with  $e \sim 0.014$ , and the Lense-Thirring drag of the perigee of LAGEOS II is almost twice as large in magnitude as that of LAGEOS. Over about 4 years, we obtained a root mean square of the residuals of the LAGEOS II perigee of about 25 mas [6], whereas the total Lense-Thirring effect on the perigee is, over 4 years,  $\cong -228$  mas.

To precisely quantify and measure the gravitomagnetic effects we have introduced the parameter  $\mu$  that is by definition 1 in general relativity [1] and zero in Newtonian theory.

The main error in this measurement is due to the uncertainties in the Earth's even zonal harmonics and their time variations. The unmodeled orbital effects due to the harmonics of lower order are comparable to, or larger than, the Lense-Thirring effect. However, by analyzing both the JGM-3 and the EGM-96 models with their uncertainties in the even zonal harmonic coefficients and by calculating the secular effects of these uncertainties on the orbital elements of LAGEOS and LAGEOS II, we find [4] that the main sources of error in the determination of the Lense-Thirring effect are concentrated in the first two even zonal harmonics,  $J_2$  and  $J_4$ . We can, however, use the three observable quantities  $\dot{\Omega}_I$ ,  $\dot{\Omega}_{II}$  and  $\dot{\omega}_{II}$  to determine  $\mu$  [4], thereby avoiding the two largest sources of error, those arising

from the uncertainties in  $J_2$  and  $J_4$ . We do this by solving the system of the three equations for the three residuals  $\delta\dot{\Omega}_I$ ,  $\delta\dot{\Omega}_{II}$  and  $\delta\dot{\omega}_{II}$  in the three unknowns  $\mu$ ,  $J_2$  and  $J_4$ , obtaining:

$$\begin{aligned} & \delta\dot{\Omega}_{LAGEOSI}^{Exp} + c_1 \delta\dot{\Omega}_{LAGEOSII}^{Exp} + c_2 \delta\dot{\omega}_{LAGEOSII}^{Exp} = \\ & = \mu (31 + 31.5 c_1 - 57 c_2) mas/yr + other\ errors \cong \mu (60.2 mas/yr), \end{aligned} \quad (3)$$

where  $c_1 = 0.295$  and  $c_2 = -0.35$ . Equation (3) for  $\mu$  does not depend on  $J_2$  and  $J_4$  nor on their uncertainties; thus, the value of  $\mu$  that we obtain is unaffected by the largest errors, which are due to  $\delta J_2$  and  $\delta J_4$ , and is sensitive only to the smaller errors due to  $\delta J_{2n}$ , with  $2n \geq 6$ .

Similarly, regarding tidal, secular, and seasonal changes in the geopotential coefficients, the main effects on the nodes and perigee of LAGEOS and LAGEOS II, caused by tidal and other time variations in Earth's gravitational field [4, 5, 14], are due to changes in  $J_2$  and  $J_4$ . However, the tidal errors in  $J_2$  and  $J_4$  and the errors resulting from other unmodeled, medium and long period, time variations in  $J_2$  and  $J_4$ , including their secular and seasonal variations, are eliminated by our combination of residuals of nodes and perigee. In particular, most of the errors resulting from the 18.6- and 9.3-year tides, associated with the lunar node, are eliminated in our measurement. An extensive discussion of the various error sources that can affect our result is given in [4, 5, 14], only a brief discussion of the error sources is given below.

Let us now report the main results of our measurements. In Fig. 1, we display the improved analysis [6] (obtained with the linear combination of the residuals of the nodes of LAGEOS and LAGEOS II and perigee of LAGEOS II according to Eq. (3)) using the static and tidal Earth gravitational model EGM-96, we also refined the non-gravitational perturbations model, the total period of observations was of 4 years, longer of about 1 year with respect to the previous observational period corresponding to ref. [5]. We only removed three small periodic residual signals and the small observed inclination residuals. The removal of the periodic terms was achieved by a least squares fit of the residuals using a secular trend and three periodic signals with 1044-, 820-, and 569-day periods, corresponding to, respectively, the nodal period of LAGEOS, and the perigee and nodal periods of LAGEOS II. The 820-day period is the period of the main odd zonal harmonics perturbations of the LAGEOS II perigee; the 1044- and 569-day periods are the periods of the main tidal



orbital perturbations, with  $l=2$  and  $m=1$ , which were not eliminated using Eq. (3). Some combinations of these frequencies correspond to the main non-gravitational perturbations of the LAGEOS II perigee. We notice that this analysis, using EGM-96 and its accurate tidal model, is substantially independent of the removed signals, whereas the previous analysis [5], was in part sensitive on the periodic terms included in the fit. In other words, our value (Fig. 1) of the secular trend does not significantly change by fitting additional periodic perturbations, and indeed, even the fit of the residuals with a secular trend only, with no periodic terms, just changes the slope by about 10 %. Nevertheless, in this case, the root mean square of the post-fit residuals increases by about four times with respect to Fig. 1.

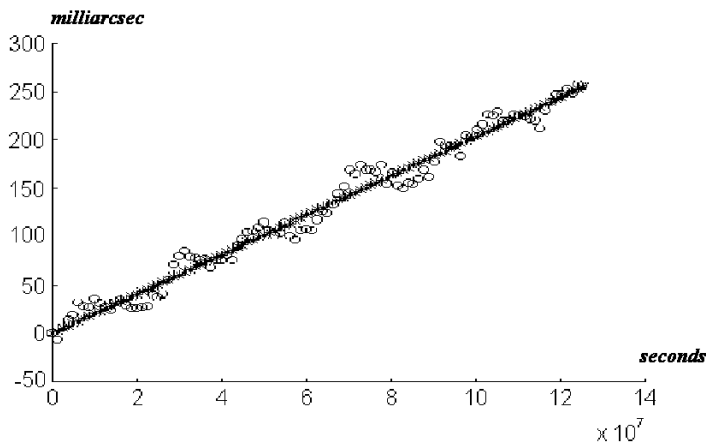


Figure 1: 1997-measurement of the Lense-Thirring effect. Combination of the residuals of the nodes of LAGEOS and LAGEOS II and perigee of LAGEOS II according to Eq. (3), using the Earth gravitational model EGM-96, over a 4-year period.

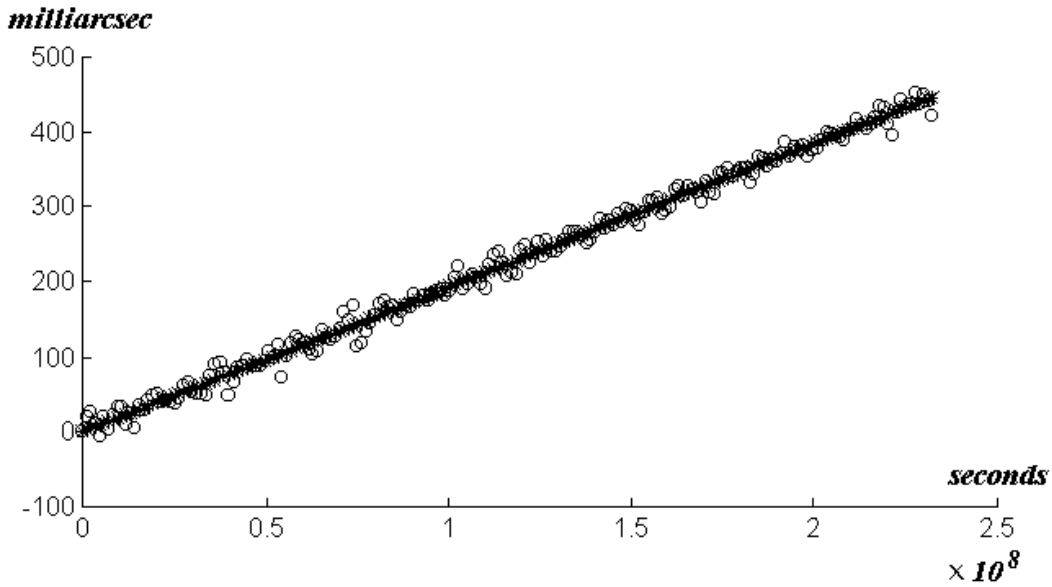
Our best-fit straight lines of Fig. 1, through the combined residuals of nodes and perigee, has a slope  $\mu^{Measured} \cong 1.1 \pm 0.03$ , where 0.03 is the standard deviation of the fit. This combined, measured, gravitomagnetic perturbation of the satellites' orbits corresponds, in a 4-year period, to about 16 m at the LAGEOS altitude, that is, about 265 mas.

The root mean square of the post-fit combined residuals corresponding to Fig. 1 is about 9 mas. Our total systematic error is estimated to be of the order of 30%-40% of  $\mu_{GR}$  corresponding to the previous analyses of ref. [5], and of the order of 20%-25% of  $\mu_{GR}$  corresponding to Figure 1 [6].

Using the JGM-3 covariance matrix, we found the errors due to the uncertainties in the even zonal harmonics  $J_{2n}$ , with  $2n \geq 6$ , to be:  $\delta \mu^{even\ zonals: J_{2n} \geq J_6} \lesssim 17\%$  of  $\mu_{GR}$ , and using the EGM-96 covariance matrix:  $\delta \mu^{even\ zonals: J_{2n} \geq J_6} \lesssim 13\%$

of  $\mu_{GR}$ . The errors in the modeling of the perigee rate of LAGEOS II due to the uncertainties in the odd zonal harmonics  $J_{2n+1}$  are, with EGM-96:  $\delta \mu^{odd\ zonals} \lesssim 2\%$  of  $\mu_{GR}$ . Using the EGM-96 tidal model, we estimated the effect of tidal perturbations and other variations of Earth gravitational field to be  $\delta \mu^{tides + other\ variations} \lesssim 4\%$  of  $\mu_{GR}$ . On the basis of analyses [14, 22] of the non-gravitational perturbations — in particular, those on the perigee of LAGEOS II — we found  $\delta \mu^{non-gravitational} \lesssim 13\%$ - $20\%$  of  $\mu_{GR}$ , including uncertainties in the modeling of the satellites' reflectivities, and the error due to uncertainties in the orbital inclinations of LAGEOS and LAGEOS II was estimated to be  $\delta \mu^{inclination} \lesssim 5\%$  of  $\mu_{GR}$ .

Taking into account all of these error sources, we arrived at a total root-sum-square error  $\lesssim 20\%$ - $25\%$  of  $\mu_{GR}$ . Therefore, over an observational period of 4 years and using EGM-96, we determined  $\mu^{Measured} = 1.1 \pm 0.25$ , where 0.25 is the estimated total uncertainty due to all the error sources.



### 2002-Measurement of the Lense-Thirring Effect

Figure 2: *Latest, 2002, measurement of the Lense-Thirring effect using LAGEOS and LAGEOS II, obtained by only modeling the radiation pressure coefficient of LAGEOS II, over nearly 8 years of data. The best-fit line shown through these combined residuals has a slope of about 1, with standard deviation 0.02. The total estimated systematic error is about 0.2. The total measured signal is nearly 440 milliarcsec and the RMS of the post-fit residuals about 10 milliarcsec.*

We finally briefly report on our latest, 2002, measurement of the Lense-Thirring effect over 7.3 years of data of LAGEOS and LAGEOS II, i.e. over an observational time nearly double than the longer period of our previous analyses, obtained by only modeling the radiation pressure coefficient of LAGEOS II (see Fig. 2) [7].

This recent measurement fully confirms and improves our previous results: the Lense-Thirring effect exists and its experimental value,  $\mu \cong (1 \pm 0.02) \pm 0.2$  (where  $\pm 0.02$  is the standard deviation of the fit and  $\pm 0.2$  is the estimated total systematic error), fully agrees with the general relativity prediction of frame-dragging. It is important to notice that: (1) in the analysis corresponding to Fig. 2 we only modeled on LAGEOS II the radiation pressure coefficient of the satellite, i.e. the reflectivity coefficient,  $C_R$ , and no other parameters such as the along-track accelerations as in our previous analyses corresponding to Fig. 1 and ref. [5, 6]; (2) the RMS of the residuals corresponding to Fig. 2 is about 10 milliarcsec whereas the total measured signal is about 440 milliarcsec, and finally (3) the quality of the fit and of the corresponding measurement can be further improved by further reducing the RMS of the 15-day fits (corresponding to each point of Fig. 2) with further processing of the data using GEODYN/SOLVE, thus further reducing the RMS of the final fit of Fig. 2.

*In conclusion, the Lense-Thirring effect exists and its experimental value,  $\mu \cong 1 \pm 0.2$ , fully agrees with the prediction of general relativity [7].*

## References

1. I. Ciufolini and J.A. Wheeler, *Gravitation and Inertia* (Princeton University Press, Princeton, New Jersey, 1995).
2. C. M. Will, in *Living Reviews in Relativity*, Max Planck Inst. for Grav. Phys.–Albert Einstein Inst., Germany, 11 May 2001: [www.livingreviews.org/Articles/Volume4/2001-4will](http://www.livingreviews.org/Articles/Volume4/2001-4will).
3. J. Lense and H. Thirring, *Phys. Z.* **19**, 156 (1918); see also English translation by B. Mashhoon, F.W. Hehl, D.S. Theiss, *Gen. Relativ. Gravit.*, **16**, 711 (1984).
4. I. Ciufolini, *Nuovo Cimento A* **109**, 1709 (1996).
5. I. Ciufolini et al., *Nuovo Cimento A* **109**, 575 (1996). — et al., *Class. and Quantum Grav.* **14**, 2701 (1997), see also — et al., *Europhys. Lett.* **39**, 35 (1997).

6. I. Ciufolini, E. C. Pavlis, et al. *Science*, **279**, 2100 (1998).
7. I. Ciufolini, E. C. Pavlis and R. Peron, to be published (2002).
8. C. W. F. Everitt, in *Experimental Gravitation*, ed. B. Bertotti (Academic Press, New York, 1974), p. 331–360.
9. I. Ciufolini and F. Ricci, *Class. and Quantum Grav.* **19**, 3863 (2002). I. Ciufolini and F. Ricci, *Class. and Quantum Grav.* **19**, 3875 (2002).
10. J. M. Cohen and B. Mashhoon, *Phys. Lett. A* **181** 353 (1993). See also: B. Mashhoon, Gronwald and Theiss, *Ann. Phys* **8** 135 1999.
11. A. Tartaglia, Online preprint (2000): <http://babbage.sissa.it/abs/gr-qc/0001080>. — *Class. and Quantum Grav.* **17** 783 (2000).
12. A. D. Biggs and I. W. A. Browne, in *International Astronomical Union Symposium no. 205* (England, August 2000).
13. I. Ciufolini, A. Paolozzi, et al. *LARES phase A study for ASI* (1998).
14. I. Ciufolini, *Phys. Rev. Lett.* **56**, 278 (1986). — *Int. J. Mod. Phys. A* **4**, 3083 (1989). See also: B. Tapley, — et al. *NASA-ASI Study on LAGEOS III*, CSR-UT publication n. CSR-89-3, Austin, Texas (1989).
15. J.J. Degnan and E.C. Pavlis, *GPS World*, **5**, 62 (1994).
16. D. McCarthy, *The 1996 IERS Conventions* (Observatoire de Paris, Paris, 1996).
17. F.G. Lemoine, et al., in Proceedings of the 1997 Institute of Astronomy and Geophysics Scientific Assembly, Rio de Janeiro, Brazil, Sept. 5-9, 1997.
18. D.P. Rubincam, *J. Geophys. Res.*, **93** (B11), 13803 (1988). — *J. Geophys. Res.*, **95** (B11), 4881 (1990). — and A. Mallama, *J. Geophys. Res.*, **100** (B10), 20285 (1995). C.F. Martin and —, *J. Geophys. Res.*, **101** (B2), 3215 (1996).
19. P. Farinella, D.V.Y. Vokrouhlicky, F. Barlier, *J. Geophys. Res.*, **101** (B8), 17861 (1996).
20. R.S. Gross, *J. Geophys. Res.*, **101** (B4), 8729 (1996).
21. D.E. Pavlis, et al. *GEODYN II, Operations Manual*, 3, (1997).
22. D. M. Lucchesi, Part I: *Plan. and Space Science*, **49**, 447 (2001); Part II: to appear in *Plan. and Space Science* (4 July 2002).